Analyzing the Hydrodynamic and Crowding Evolution of Aqueous Hydroxyapatite-Gelatin Networks: Digging Deeper into Bone Scaffold Design Variables

Javier Sartuqui, Noelia D' Elía, A. Noel Gravina, Paula V. Messina
Department of Chemistry, Universidad Nacional del Sur, (8000) Bahía Blanca, Argentina, INQUISUR-CONICET

Received 24 November 2014; revised 5 March 2015; accepted 6 March 2015
Published online 18 March 2015 in Wiley Online Library (wileyonlinelibrary.com). DOI 10.1002/bip.22645

ABSTRACT:

The hydration of the polypeptide network is a determinant factor to be controlled on behalf of the design of precise functional tissue scaffolding. Here we present an exhaustive study of the hydrodynamic and crowding evolution of aqueous gelatin-hydroxyapatite systems with the aim of increasing the knowledge about the biomimesis of collagen mineralization; and how it can be manipulated for the preparation of collagenous derived frameworks with specific morphological characteristics. The solution's density and viscosity evaluation measurements in combination with spectroscopic techniques revealed that there is a progressive association of protein chain that can be influenced by the amount of hydroxyapatite nanorods. Gelatin and additives' concentration effect on the morphology of the gelatin scaffolds was investigated. Transverse and longitudinal sections of the obtained scaffolds were taken and analyzed using optical microscopy. It can be seen that the porous size and shape of gelatin assemblies can be easily adjusted by controlling the gelatin/HAp ratio in the solution used as template in agreement with our statement. *Biopolymers 103: 393–405, 2015.*

Keywords: *gelatin; hydroxyapatite; scaffolds; intrinsic viscosity; spectroscopic methods*

This article was originally published online as an accepted preprint. The "Published Online" date corresponds to the preprint version. You can request a copy of any preprints from the past two calendar years by emailing the Biopolymers editorial office at biopolymers@wiley.com.

INTRODUCTION

Calcified tissue, such as long and jaw bones are considered a hierarchically structured nanocomposite of a Type I collagen (COL)-based soft hydrogel template and hydroxyapatite (HAp) nanocrystals, $Ca_{10}(PO_4)_6(OH)_2$.[1] Therefore, such constituents are the natural choice of structural units for scaffolding construction in bone replacing therapies. One of the underlying hypotheses in collagen research is that evolutionary bioengineering will produce a material with the ideal properties to repair existing bone defects and/or to generate new bone.[2–4] On the basis of such concepts, the synthesis of COL-HAp composites has been intensively studied in the last 2 decades. Numerous studies[5–11] have successfully demonstrated that the incorporation of calcium phosphate minerals within a collagen matrix is possible; and they also contributed significantly to the understanding of biomimetic collagen mineralization process.[3,4] Nevertheless, the ability to replicate the intricate patterns of the nanocrystalline assembly at the intrafibrillar levels has been elusive.[4] When mineralization is under strict biological control calcium-deficient apatites are deposited in a nanocrystalline form at the intrafibrillar and extrafibrillar spaces

Additional Supporting Information may be found in the online version of this article.

Correspondence to: Paula V. Messina; e-mail: pmessina@uns.edu.ar

Contract grant sponsor: Universidad Nacional del Sur
Contract grant number: PGI-UNS 24/Q064
Contract grant sponsor: Concejo Nacional de Investigaciones Científicas y Técnicas de la República Argentina
Contract grant number: PIP–11220130100100CO
Contract grant sponsor: CONICET, CONICET

associated with the collagen assembly. Regulation of calcium phosphate phase deposition during biomineralization is believed to exhibit two major characteristics: (i) the sequestration of the calcium and phosphate ions into nanoscopic entities known as amorphous calcium phosphate and; (ii) the templating of mineral nucleation, crystal growth and orientation through fibrous-hydrated proteins networks.[4] Hartgerink et al.[12] evaluated the self-assembly and mineralization of peptide nanofibers and established that, although the mechanism is still unclear, orientation of crystalline nuclei, and the subsequent crystal growth are not random, being controlled by the peptide hydrated network. Meanwhile, Magne et al.[13] studied the evolution of the Type I collagen and nonstoichiometric apatite constituents of dentin, showing that collagen fibrils became less and less hydrated, suggesting that intrafibrillar mineralization partially dehydrates the collagen fibers. In previous works[14,15] we have manipulated protein hydrogels as biological scaffolding and also a similar methodology[16] was utilized to construct bioactive and biocompatible structured networks based on bone-like hydroxyapatite nanorods. The existence of a hydrated protein network seems to be determinant in the collagen's mineralization process and is a parameter to take into account when selecting the appropriate synthesis conditions for the preparation of mineralized scaffolds based on proteins. Taken into account these considerations, in this work we prepared different gelatin-HAp self-assembly models to evaluate the effect of HAp crystals on the hydrodynamic and crowding effect on the collagenous gel structure. HAp nanorods[16] with analogous composition, size, and shape of bone-like minerals were used as the biogenic apatite source. Collagen is replaced by its denaturalized form gelatin (GEL), because of its poor commercial sources definition that makes it difficult to follow up on well controlled processing.[17–19] Viscosity and density measurements were analyzed to evaluate the effect of HAp nanocrystals incorporation on the GEL structured network organization; parameters such as intrinsic viscosity $[\eta]$, and Huggins coefficient (K_H) were analyzed to understand the behavior of the GEL hydrodynamic environment and its effect on the protein system association. In addition, the effect of HAp on gelatin conformation was investigated by spectroscopic techniques, confirming an intra-association of protein chains assembled with the addition of nanorods. The templating activity of GEL-HAp networks was analyzed ratifying that the solution organization can be transferred to the final morphology of the materials prepared from them. The analysis of crystal and biological hydrogels interactions is a versatile platform to model the intricate biological collagen mineralization. The obtained results can provide new insight into the basic process of collagen mineralized tissues formation and lead to the development of new bio-inspired nanostructured material for hard tissue repair and regeneration.

RESULTS AND DISCUSSION

Hydrodynamic Environment: Intrinsic Viscosity Analysis

Viscosity of a protein water solution is deeply related to the hydrodynamic properties, depending on the intrinsic biopolymer characteristics (such as molecular mass, volume, size shape, surface charge, deformation feasibility, and amino acid content) and on external stimuli (such as pH, temperature, ionic strength, solvent effect, etc.) This property's measurement and the parameters' interpretation derived from its analysis provided a clear picture of the macromolecule structured network organization.[20,21] The viscosity of a macromolecular solution, η, can be related to the solvent viscosity, η_0, and to the concentration of the protein, C, in g/mL by a power series[22]:

$$\eta=\eta_0\left(1+k_1C+k_2C^2+k_3C^3+\cdots\right) \tag{1}$$

where k_1 is related to the contribution of individual protein molecules while k_2 and higher order coefficients are associated to the effects from interactions of 2, 3, or more protein molecules. The constant k_1, is also known as the intrinsic viscosity $[\eta]$ and Eq. (1) can be rewritten to obtain an expression of specific viscosity/concentration ratio as a function of the solution concentration,[23] more details in ESM:

$$\frac{\eta_{sp}}{C}=[\eta]+k_2'[\eta]^2C+k_3'[\eta]^3C^2+k_4'[\eta]^4C^3+\ldots \tag{2}$$

where $\eta_{sp}=\eta_r-1$ is the specific viscosity and $\eta_r=\eta/\eta_0$ is the relative viscosity. Intrinsic viscosity, $[\eta]$, is a measure of a polymer's ability to increase the solvent's viscosity and contains information about the macromolecular shape, flexibility, and (for nonspherical particles) the molar mass.[23] It can be experimentally obtained by extrapolating protein concentration to zero as:

$$[\eta]=\lim_{\eta_{sp}\to 0}{}^{\eta_{sp}}/_{C} \tag{3}$$

When association is discarded, Einstein's viscosity law is valid, thereby as all the dissolved chains are in isolated state, monodisperse polymer's relative viscosity should be:

$$\eta_r=1+[\eta]C \tag{4}$$

and $[\eta]$ can be evaluated from viscosity measurements at finite concentrations applying diverse linear extrapolation methods to infinite dilution,[24–26] such as Huggins' equation[27]:

$$\eta_r=1+[\eta]C+K_H[\eta]^2C^2 \tag{5}$$

where, $K_{H,}$ is the Huggins coefficient. Comparing Eqs. (2) and (5), the Huggins coefficient is the numerical coefficient of the

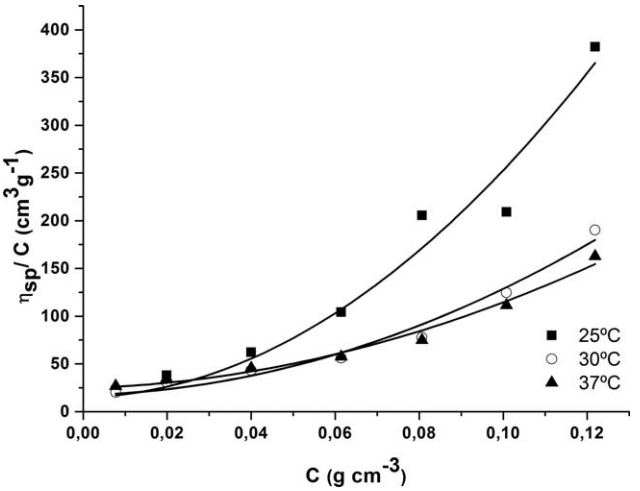

FIGURE 1 Variation of η_{sp}/C versus gelatin solution concentration, C, at different temperatures.

second term in the expansion of η_{sp}/C in terms of C, Eq. (2). Since the relative populations of the several species depend on higher powers of concentrations than the first, their presence must contribute to the k_i terms. These populations may be formally expressed in terms of equilibrium constants. Considering the following equilibriums of protein molecules (P) with identical molar self-association constant, K_a, for all the equilibriums:

$$P + P \overset{K_a}{\leftrightarrow} P_2$$

$$P_2 + P \overset{K_a}{\leftrightarrow} P_3$$

$$\vdots$$

$$P_{i-1} + P \overset{K_a}{\leftrightarrow} P_i,$$

and that any deviation from Eq. (4) is due to macromolecular self-association or cluster formation. Then, instead of the conventional Huggins equation [Eq. (5)], the $\eta_{r,\,true}$ of a polymer solution can be represented by:

Table I Coefficients of the Polynomial Eq. (2): $\frac{\eta_{sp}}{C} = P_1 + P_2C + P_3C^2 + P_4C^3 + \cdots$, where $P_1 = [\eta]$, $P_2 = k_2'[\eta]^2$, $P_3 = k_3'[\eta]^3$, $P_4 = k_4'[\eta]^4$ and so on

	P_1/cm^3 g^{-1}	P_2/cm^{6}g^{-2}	P_3/cm^{9}g^{-3}	P_4/cm^{12}g^{-4}	P_5/cm^{15}g^{-5}	R^2
25°C						
GEL	14.9	105.4	22,729			0.99877
			Hap			
+20mg	16.4	130.5	1,286	82373		0.99879
+30mg	6.9	15.5	45,744.8	-8.22×10^5	4.5×10^6	0.99154
+50mg	11.3	60.4	3.17×10^4	-5.9×10^5	3.3×10^6	0.99478
			Ca^{2+}			
+20mg	18.6	100.2	2.6×10^4	-4.6×10^5	3.3×10^6	0.99879
+30mg	11.3	55.9	1.7×10^4	-2.6×10^5	1.6×10^6	0.99979
+50mg	16.4	102.9	-4.7×10^3	2.5×10^4	-1.7×10^6	0.99225
			30°C			
GEL	17.5	98	10133.2			0.98998
			Hap			
+20mg	17.6	110.9	2304	32506.7		0.99975
+30mg	12.05	100.2	2.5×10^4	-4.5×10^5	2.3×10^6	0.98998
+50mg	9.0	45.7	2.5×10^4	-4.2×10^5	2.1×10^6	0.99387
			Ca^{2+}			
+20mg	14.4	66.4	3.2×10^4	-6.3×10^5	3.9×10^6	0.99678
+30mg	9.13	13.4	2.7×10^4	-5.3×10^5	3.3×10^6	0.99298
+50mg	11.9	34	1.1×10^3	-1.6×10^4	1.0×10^6	0.99837
			37°C			
GEL	24.6	130.4	7990			0.99678
			Hap			
+20mg	19.3	122.2	4323	7949.7		0.98997
+30mg	18.4	219.3	2.4×10^4	-4.7×10^5	2.5×10^6	0.99126
+50mg	6.10	20.21	3.1×10^4	-5.4×10^5	2.7×10^6	0.99689
			Ca^{2+}			
+20mg	22.2	45.4	2.7×10^4	-5.5×10^5	3.7×10^6	1
+30mg	14.4	19.1	1.5×10^4	-2.4×10^5	1.4×10^6	0.99899
+50mg	19.5	45.4	-9.2×10^3	3.4×10^4	-2.4×10^6	0.97309

$$\eta_{r,true} = 1 + [\eta]C + 6K_m[\eta]C^2 \quad (6)$$

where K_m is the apparent self-association constant. K_m is related to the size and interactions between polymer chains in solution and numerically correlates with Huggins coefficient (K_H) and $[\eta]$ as follows[28]:

$$K_m = \frac{K_H[\eta]}{6} \quad (7)$$

The dependence of (η_{sp}/C) versus pure gelatin solution concentration (C) is shown in Figure 1**,** similar results were obtained after the addition of HAp nanorods and Ca^{2+} (see the electronic Supporting Information, ESM). A direct relationship between η_{sp}/C versus C was obtained and no anomalous behavior indicating electroviscous or salting-out effects became evident.[23,29] It can be observed that η_{sp}/C increases very rapidly at higher concentrations and the graphs present a positive curvature. At higher concentration of interest, the higher order terms of the power series in Eq. (2) will dominate, and the virial coefficients, which are related to molecular interactions will significant contribute to the viscosity. Due to polymer association, it is not suitable the use of linear equations mentioned above and the values of $[\eta]$ and K_H must be obtained from the application of the general equation [Eq. (2)]; the results of polynomial regression analysis are listed in Table I**.** It can be observed that GEL solutions without the presence of additives are well described by a second order polynomial equation; however, the addition of HAp nanorods or Ca^{2+} ions increases the polynomial order to three and four, respectively. The incorporation of additives in all cases would increase the polymer association; it specific effect on the macromolecular network is analyzed below.

The Role of HAp on $[\eta]$, K_H, and K_m Parameters

The obtained $[\eta]$, K_H, and K_m parameters are summarized in Table II. Huggins coefficient (K_H) is characteristic of hydrodynamic and thermodynamic polymer interactions[30] and is a decreasing function of the viscosity radius expansion factor, α_n:

$$\alpha_n = \left([\eta]/[\eta]_0\right)^{1/3} \quad (8)$$

where $[\eta]_0$ and $[\eta]$ are the intrinsic viscosity for chains unperturbed by the excluded–volume effect and for chains perturbed by this effect in good solvent systems respectively. The K_H should be lower in good solvents where polymer−solvent interactions are favored. For polymers in good solvents $K_H \cong 0.33$ while values larger than 0.5−1 are typically found in poor solvents.[31] These last values are attributed to polymer chain association.[30] The value of K_H for pure gelatin solutions at $T = 25°C$ is almost 0.5 and decreases with the increment of T. At $T > 25°C$, protein−solvent interactions are favored and the buffer solution acts as a good solvent. Accordingly to Eq. (7) K_H has a direct relationship with polymer association and an inverse correlation with intrinsic viscosity; also intrinsic viscosity direct depend on polymer shape and excluded volume.[21] The decrease in K_H values with T in pure gelatin solutions may be due to polymer dissociation simply because of an increase in Brownian motion (slight decrease of K_m values) and protein excluded volume due to the association of carboxyl and amino groups with solvent by hydrogen bonds (increasing $[\eta]$ values). The addition of 20 mg of HAp nanorods at $T \leq 30°C$ did not affect the values of K_H, K_m, and $[\eta]$ in comparison with pure gelatin buffer solutions at identical thermal conditions. This fact would suggest that there was not an extra- structuring effect of the solution due to HAp incorporation. However at $T = 37°C$, there was a significant decrease of $[\eta]$ complemented with an increase of K_m and K_H values. Evidently the presence of HAp nanorods (even in small amounts) generates

Table II Gelatin Solutions Viscosity Data

	$[\eta]$/cm^{3}g^{-1}	$[\eta]_{dyn}$/cm^{3}g^{-1}	K_H	K_m/cm^{3}g^{-1}
25°C				
GEL	14.9	15.2	0.474	1.177
		Hap		
+20 mg	16.4	16.7	0.484	1.324
+30 mg	6.9	7.2	0.321	0.372
+50 mg	11.3	11.5	0.474	0.889
		Ca^{2+}		
+20 mg	18.6	18.8	0.291	0.899
+30 mg	11.3	11.6	0.430	0.810
+50 mg	16.4	16.7	0.386	1.053
		30°C		
GEL	17.5	17.8	0.322	0.936
		Hap		
+20 mg	17.6	17.9	0.357	1.047
+30 mg	12.1	12.3	0.690	1.386
+50 mg	9.0	9.3	0.568	0.849
		Ca^{2+}		
+20 mg	14.4	14.7	0.321	0.769
+30 mg	9.1	9.4	0.160	0.245
+50 mg	12	12.3	0.238	0.474
		37°C		
GEL	24.6	24.8	0.216	0.884
		Hap		
+20 mg	19.3	19.6	0.327	1.053
+30 mg	18.4	18.7	0.648	1.986
+50 mg	6.1	6.4	0.539	0.548
		Ca^{2+}		
+20 mg	22.2	22.5	0.092	0.340
+30 mg	14.4	14.7	0.092	0.221
+50 mg	19.5	19.8	0.119	0.387

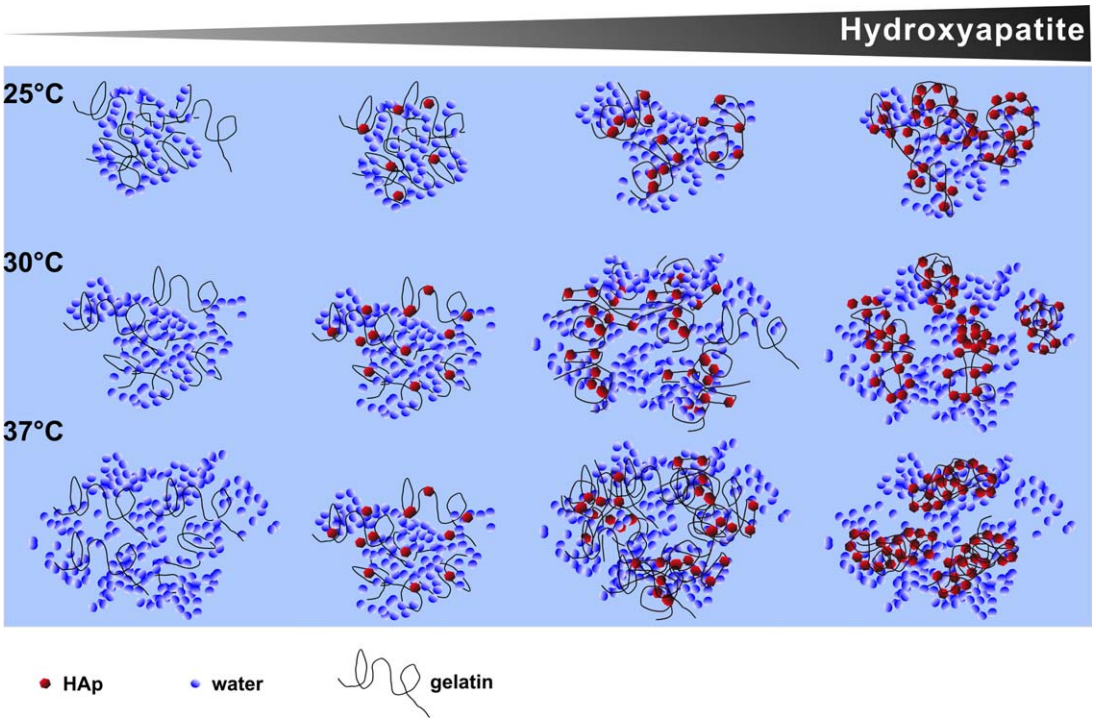

SCHEME 1 Schematic representation of aqueous hydroxyapatite-gelatin networks crowding evolution.

a kind of association that overcomes the molecular motion created by the increment of *T*. The incorporation of 30 mg of HAp nanorods into buffer gelatin solutions at 25°C causes a decrease of Huggins coefficient, $K_H = 0.321$. This effect occurs simultaneously with a high decrease of K_m and $[\eta]$ values. The addition of a rather larger amount of nanorods generates a decrease in protein interchain association and in the protein chain excluded volume; that would be possible if protein molecules were coiling on themselves or around the HAp nanorods forming small aggregates. In these conditions and at $T > 25°C$, K_m, and $[\eta]$ values increase probably because of the effect of thermal motion causing the small preformed aggregates collide to form larger ones. Because of the increment of K_H values, it can be noticed that the effect of the protein aggregates association would exceed the increase of excluded volume. The addition of a larger amount of nanorods (50 mg) generates a simultaneous decrease in the association among the protein chains and in their excluded volume. This effect increases with the increment of *T* and it is presumably due to an intensification of gelatin chains association around HAp crystals. In industrial gelatin processes, many collagens' peptides bonds are broken, and a big number of dissociated groups as —COOH and $—NH_2$ are obtained. At pH = 4, lower than gelatin's IP, protein molecules have an overall positive charge. It was demonstrated that such groups can interact with the –OH groups of glass,[28] and probably they have the same behavior with the hydroxyls groups of the overall negative charged HAp crystals (IP = 3.1–3.4).[32] A schematic representation of GEL association after the addition of HAp nanorods can be seen in Scheme 1.

The presence of divalent cation (Ca^{2+}) induces aggregation of synthetic polyelectrolytes[33,34] including gelatin.[35] To confirm the effect of hydroxyapatite nanorods as a whole on gelatin association, and to discard the Ca^{2+} responsibility in the protein assembly, the effect of the incorporation of different amounts of Ca^{2+} on the hydrodynamic behavior of gelatin solutions was evaluated. The addition of 20 mg of Ca^{2+} causes a decrease of K_H values below 0.33, and this effect is greater with the increment of *T*. Many phenomena in colloid polymer and interface science involving electrolytes show pronounced ion specificity. More than a century ago, Franz Hofmeister noted a particular ordering of ions in the ability of salts of a common counterion to precipitate egg-white proteins.[36] It was thought that an ion's influence on macromolecular properties was caused at least in part by "making" or "breaking" bulk water structure. The ions called kosmotropes, which were believed to be "water structure makers" are strongly hydrated and have stabilizing effects on proteins. On the other hand, ions called chaostropes were water structure breakers and are known for destabilizing folded proteins.[37] Ca^{2+} is a chaostrope ion; its presence in solution destabilizes the gelatin intramolecular interactions, increases gelatin chains' random and

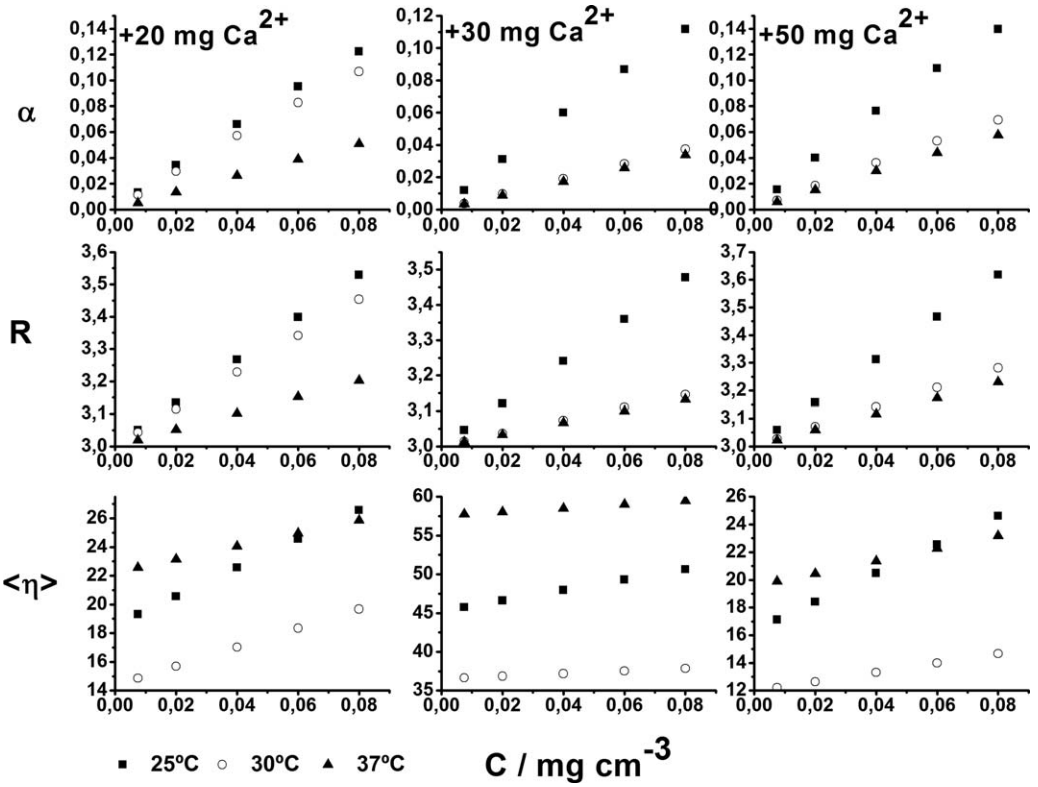

FIGURE 2 Dependence of α, *R*, and $<[\eta]>$ parameters on gelatin solution concentration, *C*, after the addition of different amount of Ca^{2+}.

disentanglement, and breaks the water structure. All mentioned effects favored solvent–Ca^{2+}–protein contacts decreasing interchain protein association (significant decrease of K_m values) and slightly increasing in hydration volume. Both factors cause a decrease in K_H. Although gelatin at pH = 4 has an overall positive charge, we are working near the isoelectric point so that under these conditions there are many -COOH groups to bind calcium ion by electrostatic unions. A further increase in the amount of added Ca^{2+} (30mg) at 25°C causes a little increment of K_H value associated to a reduction in $[\eta]$ and K_m. The effect in the excluded volume is superior than the effect in protein chain association; this fact was assumed to be due to the existence of selected intramolecular connections among protein chains because of calcium ions presence. Intrachain is less effective than interchain complexation because of the chain rigidity. Temperature increase ($T > 25$°C) would augment the protein chain flexibility and the probability of intrachains' aggregation effectiveness; favoring K_H, K_m, and $[\eta]$ reduction. After the addition of large amounts of Ca^{2+} (50 mg) besides intramolecular joints, a major proportion of intermolecular cross links would appear. Thus for GEL-50 mg Ca^{2+} solution at 25°C, K_m, and $[\eta]$ parameters show a new augment. This effect persists with the subsequent increment of *T*.

Gelatin and HAp-Gelatin Systems Association

When the self-association occurs, based on Pan et al. procedure,[38] the intrinsic viscosity should be the weight average of the intrinsic viscosities of isolated chains $[\eta]$ and clusters $[\eta]_c$,

$$[\eta] = \alpha[\eta]_c + (1-\alpha)[\eta] \tag{9}$$

where α is the weight fraction of the clusters. Equation (4) can be rewritten as:

$$\eta_r = 1 + [\eta](1 + R\alpha)C \tag{10}$$

$$\text{where } R = \left([\eta]_c - [\eta]\right)/[\eta] \tag{11}$$

As it was assumed that the molar self-association constant K_a is identical for all the macromolecules equilibrium, the parameter α can be defined as[38]:

$$\alpha = \left[2(K_m C)^2 + (1 + 4K_m C)^{1/2} - 2K_m C - 1\right]/[2(K_m C)] \tag{12}$$

Protein aggregation can also be analyzed from the inspection of α, *R*, and $<[\eta]>$ parameters with the increase of protein concentration, temperature and additives, Figures 2 and 3. As we discussed previously, the aggregation of proteins chains in gelatin solutions without additives increases linearly with concentration and decreases with temperature. Both

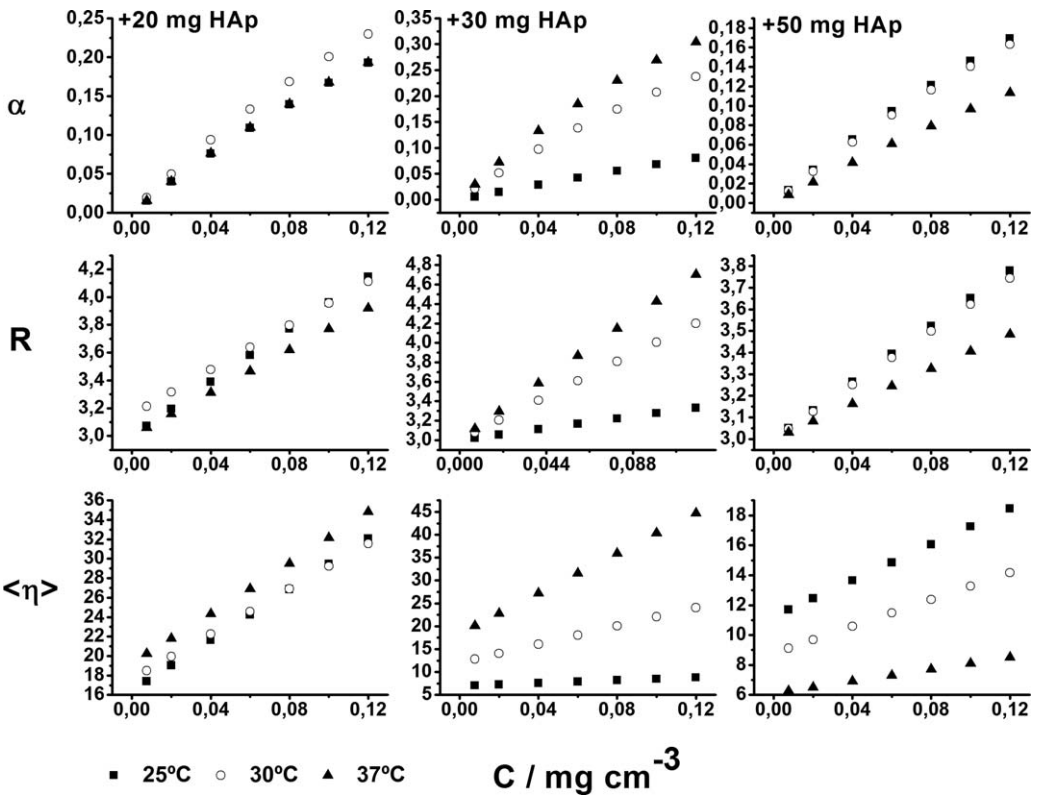

FIGURE 3 Dependence of α, R, and $<[\eta]>$ parameters on gelatin solution concentration, C, after the addition of different amount of HAp nanorods.

incorporation of HAp and Ca^{2+} intensified the temperature effect on protein association. Figures 2 and 3**,** show a great diminution of α and R parameters at 37°C after the incorporation of 20 mg of Ca^{2+} which augments with the subsequent additions of calcium ion. A similar effect can be seen after the addition of HAp. However, incorporating HAp nanorods show a different effect on α and R parameters compared with the presence of Ca^{2+}. The addition of 30 mg of HAp nanorods increases aggregation of gelatin, while the wider incorporation of this additive causes a decrease in α parameter in agreement with previously reported K_m values. The average intrinsic viscosity, $<[\eta]>$, shows a large rise with temperature increment for original gelatin solutions that decreases with the addition of 20 mg of HAp. The addition of 30 mg of HAp greatly depresses the average values of intrinsic viscosity at $T < 37$°C, which is consistent with the aggregation of the protein and the decrease of the excluded volume thereof. The situation is reversed with the addition of 50 mg of HAp, which shows that the average intrinsic viscosity falls with temperature. The presence of greater amounts of HAp nanorods, provoked an alteration in the excluded volume of the protein and thus a decrease in viscosity. There is a large decrease in the average intrinsic viscosity due to the effect of Ca^{2+} at $T = 30$°C, while it increases at 37°C. This fact confirms our previous assumption of internal interactions between protein chains due to the presence of calcium ions. At higher temperatures the chains are more flexible and these linkages are favored. However, a further increase in temperature increases the thermal agitation thus begins to prioritize interactions between protein chains. This can be clearly seen from the variation of $[\eta]_c$ (contribution to intrinsic viscosity due to the existence of protein−protein aggregates) versus protein concentration, ESM**.** The presence of protein clusters exerts a small effect on $<[\eta]>$ at 30°C, when the protein is flexible enough to fold over itself and intramolecular interactions occur.

Influence of HAp Nanorods on Hydration and Stiffness of Gelatin Networks

Hydration consists on the binding of water dipoles to ions or ionic groups, this phenomena takes place in solid substances as well as in solution. The extent of hydration can be determined and measured by the increment in weight. However, the extent of hydration in aqueous biopolymers that is accompanied by a very small change in the volume contraction of the solute and of the solvent is difficult to measure directly.

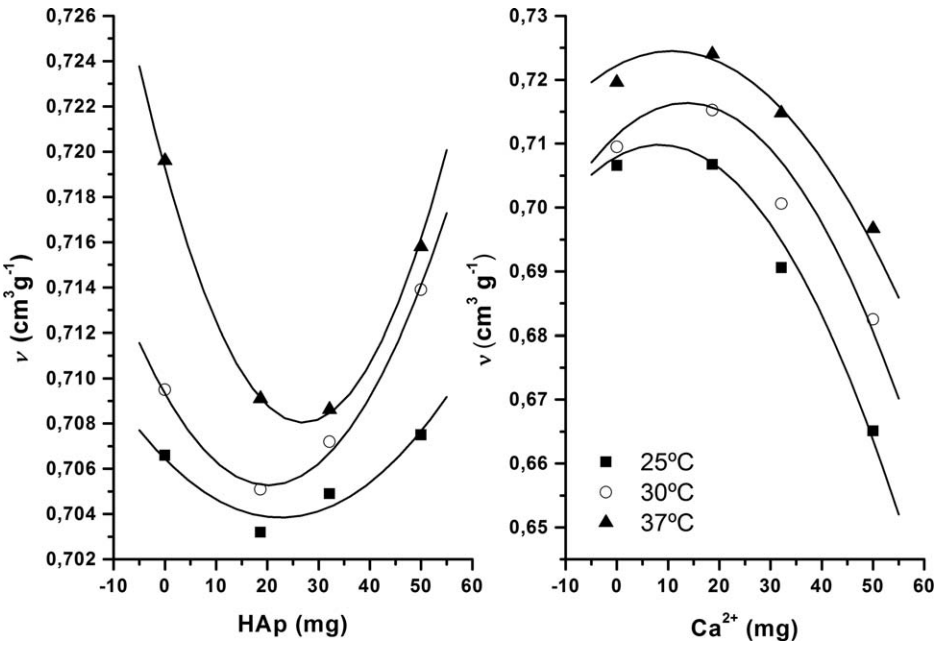

FIGURE 4 Effect of additive amount on the partial specific volume, $\bar{v}$.

Hence, it is habitual to measure the biopolymer solution's density as an independent way to evaluate the hydrodynamic behavior of protein networks. A (dynamic) intrinsic viscosity, $[\eta]_{dyn}$, is then defined[39]:

$$[\eta]_{dyn} = \{(1-\bar{v}\rho_0)/\rho_0\} + [\eta] \quad (13)$$

$$\bar{v} = \left\{\frac{1-\partial\rho/\partial C}{\rho_0}\right\} \quad (14)$$

where $\bar{v}$ is defined as the partial specific volume and corresponds to the volume occupied in solution by nonhydrated protein per gram of dry protein; ρ_0 and ρ are the solvent and solution density respectively and $[\eta]$ is the previously defined intrinsic viscosity without a density correction also known as kinematic intrinsic viscosity.[39] Figure 4 shows the variation of $\bar{v}$ vs. the amount of HAp nanorods and Ca^{2+} added to the protein solution at different temperatures. The $\bar{v}$ values always augment with temperature increment; such effect is consistent with an increase of random and disentanglement of gelatin chains. The variation of $\bar{v}$ vs. the added amount of HAp can be fitted to a parabola with a minimum at about 20 mg of HAp at 25°C and 30°C; such minimum displaces to 28 mg of HAp with the increment of *T*. The decrease of $\bar{v}$ until the addition of 20 mg HAp can be assigned to an intrachain complexation that results in the contraction of individual gelatin chains. Subsequent additions of HAp nanorods provoke an interchain complexation effect after the first intrachain complexation and the formation of larger clusters, in agreement with previously examined viscosity data. Unlike HAp addition behavior, the incorporation of Ca^{2+} causes a continuous decrease in the $\bar{v}$ parameter. Ca^{2+} complexation with —COO— groups are well documented and the "egg box model" was proposed to account for the understanding of the underlying intricacies of this binding.[40] From the molecular structure of gelatin molecules the Ca^{2+}/COOH complexation is a definite possibility and such fact can explain the reduction in $\bar{v}$ values. Generally, temperature effect on protein solutions is significant. The

Table III Variation of $\frac{dLn[\eta]}{d(\frac{1}{T})}$.

	$\frac{dLn[\eta]}{d(\frac{1}{T})}$ of GEL Solution						
		+ HAp/mg			+Ca^{2+}/mg		
T/°C		20	30	50	20	30	50
25	−18,890	−23,282	−86,889	39,590	10,562	9,513	12,576
30	−69,345	−23,282	−86,889	39,590	−801	−1,125	−721
37	−241,882	−23,282	−86,889	39,590	−12,692	−12,650	−14,584

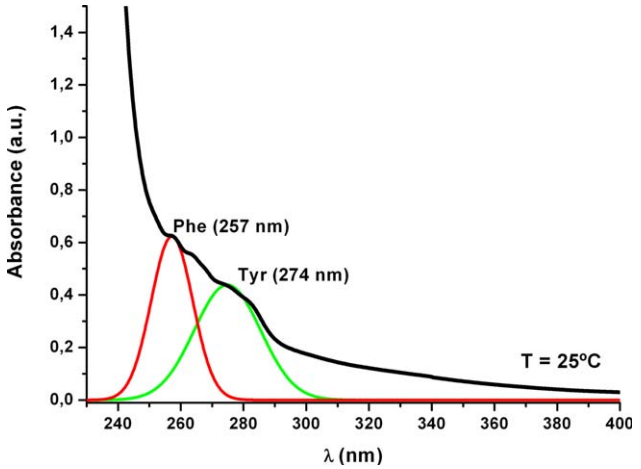

FIGURE 5 UV-vis absorption spectrum of gelatin solution at 25°C.

theoretical properties of a Newtonian fluid or a polymer liquid are consistent with the Arrhenius equation[41]:

$$\eta_{\text{apparent}} = Ae^{E_a/RT} \tag{15}$$

where A is the characteristic constant for a polymer of a specific shear rate and molecular weight, E_a is the activation energy for the flow process, R is the gas constant, and T is the absolute temperature. If the apparent viscosity, η_{app}, is replaced with intrinsic viscosity or relative viscosity, the slope $dLn[\eta]/d(1/T)$ or $dLn(\eta_r)/d(1/T)$ can also be used as an index of the resistance of a polymer to flow because it is proportional to E_a. Furthermore, the slope increases with increasing flow resistance of the polymer. Moreover, for a series of systems, increases in the flow resistance may be related to increment in their relative stiffness.[41] The variation of $dLn[\eta]/d(1/T)$ shows that the polymer rigidity decreases with temperature for pure GEL and GEL-Ca^{2+}, Table III; higher rigidity was observed in the solutions formed in Ca^{2+} environment. Such fact can be attributed to the formation of additional linkages between gelatin chains mediated by Ca^{2+} ions. A different effect can be appreciated in the presence of HAp nanorods: (i) the temperature effect on gelatin chains rigidity disappeared, (ii) a small amount addition of HAp causes a preservation of gelatin chains structure upon the temperature effect, probably due the formation of intrachain complexation, (iii) a moderate amount of HAp incorporation to GEL solution decrease the chain rigidity, probably due the intrachain formation of aggregates, and finally (iv) there is a high increment of chain rigidity due to the formation of high amount of intrachain aggregates.

Chemiluminescence Study

Changes in protein conformation, such as unfolding or aggregation generally lead to large changes in its UV-vis and fluorescence emissions. The aromatic group emissions of a native protein can be bigger or smaller than emissions in aqueous solutions. Consequently, both increase and decrease in UV intensity can occur upon a change in protein conformation.[42] To further explore the effect of hydroxyapatite incorporation in the construction of gelatin aqueous networks, we analyzed the protein's conformation variation through spectroscopic methods. A pure gelatin solution spectrum is shown in Figure 5. The UV absorption spectrum of Type-B gelatin exhibits a strong band below 240 nm that can be attributed to the nonaromatic amino acids of the structures.[43] The observed bands at the longest wavelength interval (250−300 nm) are due to the presence of aromatic amino acids. Deconvolution of absorption bands confirmed the existence of a two peak centered at 257 nm and 274 nm due to Phenylalanine and Tyrosine, that are the aromatic amino acids present in gelatin at proportions of 14 and 1.2 residues per/1000 total residues, respectively.[43] No signals were detected on spectral region beyond 300 nm

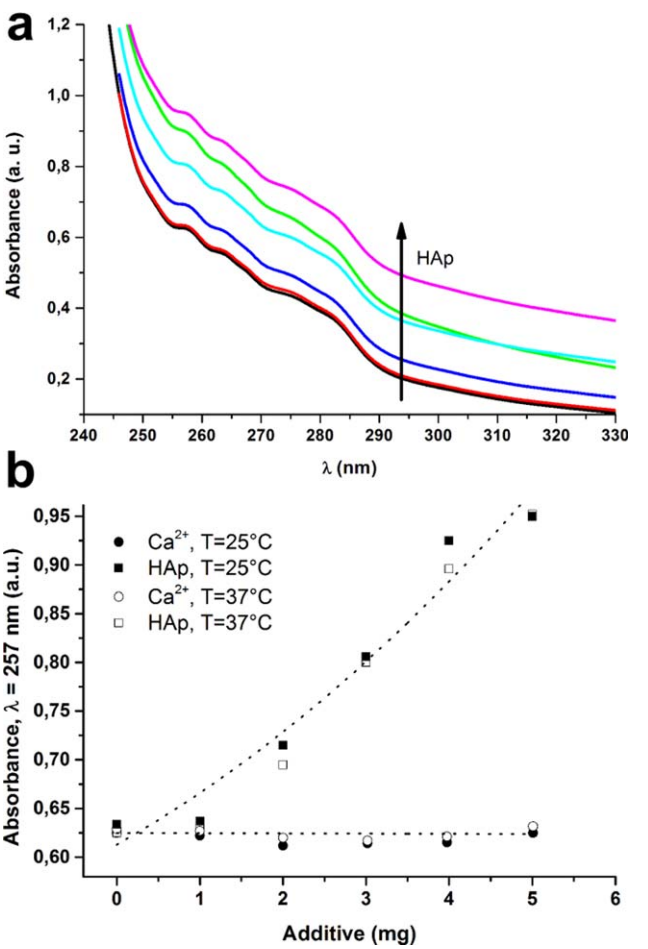

FIGURE 6 (a) UV-vis absorption spectra of gelatin solution at 25°C after incorporation of increasingly amounts of HAp nanorods. (b) Aromatic amino acids absorption dependence with the amount of additive and temperature.

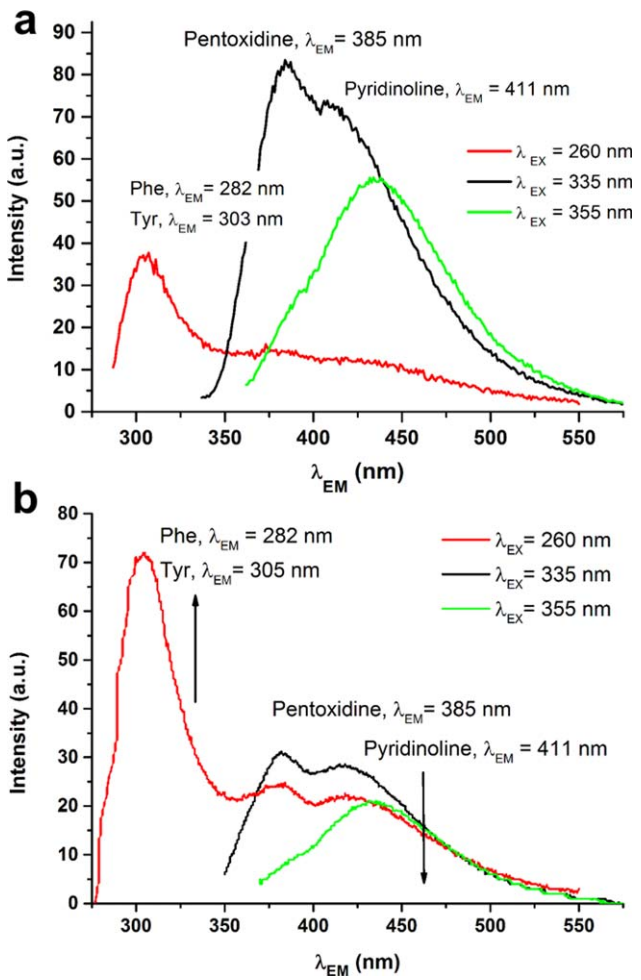

FIGURE 7 Fluorescence emission spectra of (a) gelatin and (b) gelatin plus 3 mg of HAp nanorods solutions at 25°C.

indicating that no visible absorbing oxidizing species or impurities are present. UV-vis absorption spectra of gelatin solutions after the addition of different amounts of HAp nanorods are shown in Figure 6a**.** It can be seen a radical increase of absorption emissions with the augment of HAp concentration; this effect was not advertised in the presence of Ca^{2+} and remains after a temperature increment (Figure 6b). Fluorescence emission using an excitation wavelength in the absorption region ($\lambda_{EX} = 260$ nm) generates a broad band in the (255−325 nm) wavelength range. Spectral deconvolution confirmed the presence of Phenylalanine ($\lambda_{EM} = 282$ nm) and Tyrosine ($\lambda_{EM} = 303$ nm) residues on gelatin structure. A further excitation at 335 nm and 355 nm exposed the existence of Pyridinoline ($\lambda_{EX} = 295$ nm/$\lambda_{EM} = 395$ nm)[44] and Pentoxidine ($\lambda_{EX} = 235$ nm/$\lambda_{EM} = 385$ nm)[43] groups, whose presence is associated with cross-linking of protein chains[43,44] (Figure 7a). The comparison of protein solutions fluorescence emissions before and after HAp addition indicated that there is a simultaneous increment of aromatic amino acids and a reduction of cross-link residues emissions with the addition of HAp nanorods (Figure 7b). In a hydrophobic environment (buried within the core of the protein), Tyr, and Phe have a high quantum yield and therefore a high fluorescence intensity. In contrast, in a hydrophilic environment (exposed to solvent) their quantum yield decreases leading to low fluorescence intensity. Both facts confirmed the coiling and intraassociation of protein chains with the addition of HAp.

Templating Activity of Gelatin-HAp Networks

To confirm that the effect of gelatin solution organization can be transferred to the structure of the materials prepared from them; different GEL, GEL-Ca^{2+}, and GEL-HAp solutions were cooled under −50°C during 24 h and lyophilized in a Rificor L-A-B4 lyophilizer. This technique does not require additional chemicals, relying instead on the water already present in solution/hydrogel to form ice crystals, which can be separated from the polymer by sublimation, creating a particular microarchitecture. The direction of growth and size of the ice crystals are functions of the temperature gradient and the properties of the polymer template solution.[45] By maintaining constant the temperature gradient, the structuring of the samples was considered only dependent on the properties of the solution. The effect of the gelatin and additives concentration on the morphology of the gelatin scaffolds was investigated. Transverse and longitudinal sections of the obtained framework were taken and analyzed using optical microscopy; results are shown in Figure 8**.** Cross and vertical sections of the samples are nearly analogous denoting homogeneity in dissolution. In pure GEL networks the pores, which are the result of the connective gelatin arrays, are round in shape and randomly distributed; while in the material template by GEL-Ca^{2+} and GEL-HAp most of them look similar to oblate and are arranged regularly in certain local areas. The porosity of the gelatin scaffolds increased almost linearly with the decrease in gelatin concentration. This was attributed to the effect of gelatin cross-link on the growth of ice crystals during the freeze stage. In a gelatin solution, the water molecules are separated by the macromolecules that block avoiding the concentration and organization during freezing. When the gelatin concentration increases, as discussed in section 3.1, the viscosities of the gelatin solutions augment. Therefore, for the solvent molecules (water), it is more difficult to concentrate and arrange themselves between protein chains connections, and the crystal growth is restricted. Since the ice crystals took the action of a template, their shape was imprinted in the porous gelatin scaffold after drying treatment. As a result, the micro-rods of ice crystals got thinner, and porosity decreased. A similar effect is produced when hydroxyapatite crystals or calcium ions are added to the solution. It can be

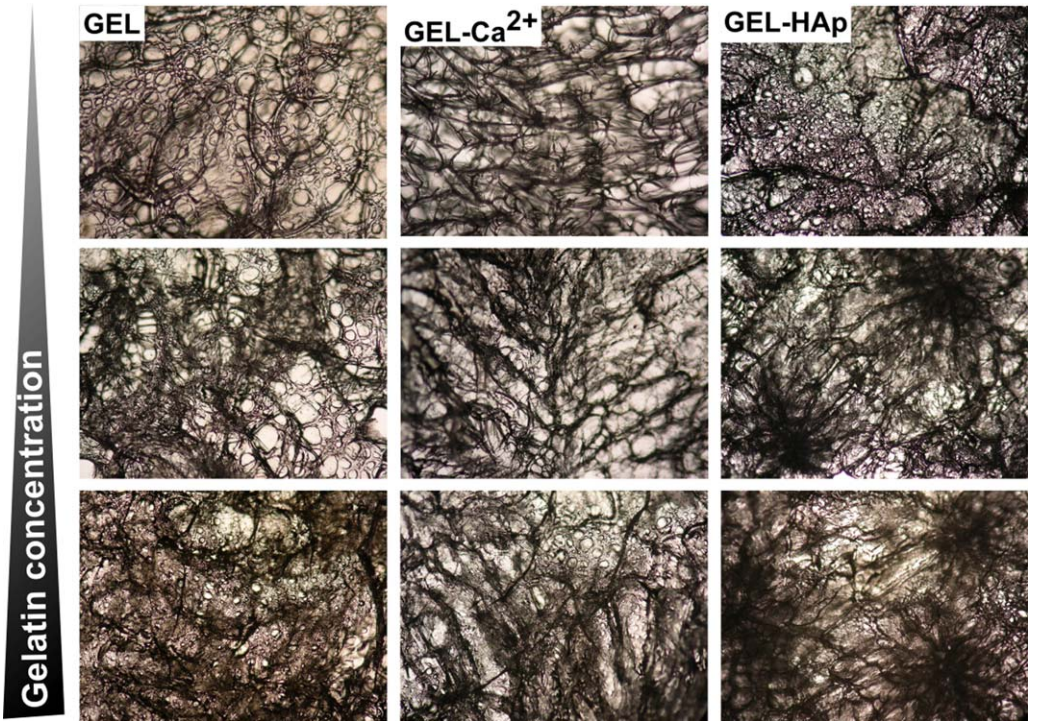

FIGURE 8 Optical microphotographs of GEL, GEL-Ca^{2+}, and GEL-HAp scaffolds longitudinal cross sections. Magnification 10×. Ca^{2+} = 50 mg, HAp = 50 mg.

observed a less cross-linked and a greater porosity structure in the samples assembled from GEL-Ca^{2+} solutions in agreement with previously discussed results that show that the presence of Ca^{2+} ions disrupt the protein chain aggregation, sections 3.2–3.4. In the GEL-HAp networks' images, a repetitive pattern of high density areas is appreciated in the material. These are consistent with the self-aggregation of the protein chains around HAp nanorods and the formation of clusters in the solution. The obtained results suggested that the porous size and shape of gelatin scaffolds can be easily adjusted by controlling the concentration of gelatin solution, Ca^{2+}, and HAp presence during its preparation and that the association of proteins not only occurs during the formation of the hydroxyapatite crystals but would be influenced by them, once crystals are formed.

CONCLUSIONS

Intrinsic viscosity data plus spectroscopic measurements were combined together to go deeper in the analysis of hydrodynamic and crowding evolution of aqueous hydroxyapatite-gelatin networks. It was determined that the continuous phase of the studied gelatin GEL solutions, water, is in dynamic equilibrium with dispersed gelatin macromolecules constituting an ensemble of physically interconnected units, which are hold together by intramolecular and intermolecular bonds. The structure of bound and interstitial water undergoes significant changes as the system structure is altered by incorporation of HAp nanocrystals affecting the hydrodynamic environment of the network and thus modulating its relaxation feature having a serious influence on the scaffold structure.

MATERIALS AND METHODS

Reagents

Hexadecyl-trimethyl ammonium bromide (CTAB, MW = 364.48 g mol^{-1}, 99%, Sigma), poly (propylene glycol) (PPG, Sigma-Aldrich, MW = 425 g mol^{-1}, δ = 1.004 g cm^{-3} at 25°C), sodium phosphate (Na_3PO_4, MW = 148 g mol^{-1}, 96%, Sigma), calcium chloride ($CaCl_2$, MW = 91 g mol^{-1}, 99%, Sigma), sodium nitrite ($NaNO_2$, MW = 69 g mol^{-1}, 97%, Sigma), acetic acid ($C_2H_4O_2$, MW = 60.05 g mol^{-1}, 99%, Sigma), sodium acetate trihydrate ($C_2H_3NaO_2 \cdot 3H_2O$, MW = 136.03 g mol^{-1}, 99%, Sigma), sodium hydroxide (NaOH, MW = 40 g mol^{-1}, 90%, Sigma), and commercial gelatin from bovine skin (Grade OR, Type B, 225 Bloom, MW ≈ 50,000 g mol^{-1}, Merck, IP = 4.5−5.6) were used without further purification. For solutions preparation, only triplet-distilled water was used.

Solutions

Totally, 0.0025−0.1000 g mL^{-1} gelatin solutions were prepared by the dissolution of the appropriate amount of commercial gelatin in 35 mL of sodium acetate buffer (pH = 4.5) at 40°C and letting it to

rest in a thermostatic bath for 24 h in order to attain the equilibrium. New sets of solutions were obtained after the addition of 20, 30, and 50 mg of HAp nanoparticles or Ca^{2+} ion to the previous described gelatin solutions with vigorous sonication.

HAp Nanoparticles

Bone-like HAp nanoparticles (7−9 nm diameter and 25−50 nm length) were prepared as described in a previous work.[16] First, 350 mL of a 3.13 m*M* CTAB aqueous solution was mixed with 20 mL of PPG and stirred at 500 rpm during 10 min. Second, 200 mL of 2*M* sodium nitrite aqueous solution and 2.2 g calcium chloride were incorporated in sequence and finally, 200 mL of 0.14*M* of Na_3PO_4 aqueous solution was added to the above mixed solution drop by drop at room temperature under magnetic stirring at 500 rpm. After the integration of all reactants, the solution was magnetically stirred for 1 h. The resulting gels were left for 24 h in an autoclave at 100°C. The obtained materials were filtered and washed with triplet-distilled water to remove impurities. Finally, surfactant was completely removed by acidic solvent extraction technique.[46,47]

Viscosity and Density Measurements

Viscosity and density measurements were performed at 25.0, 30.0, and 37.0 ± 0.1°C with a A&D Company Limited SV-10 viscometer and a Portable Density meter DMA 35N, respectively. Temperature was maintained by a thermostatic bath with recycling water throughout all the experiment. The use of a vibro-viscometer avoids the capillary adsorption effects[28] that is usually present in viscosity measurements of dilute concentration.

UV-Vis and Fluorescence Spectroscopy

UV-vis absorption spectra were recorded at 25°C and 37°C by a JASCO V-630 bio spectrophotometer provided with a temperature controller (ETCS-761 JASCO). Fluorescence emission spectra were registered at 25°C with a Varian Cary Eclipse spectrofluorometer. In both cases a 1 cm path length quartz cell was used. Buffer solution was used as blank.

Optical Microscopy

Optical microscopy was performed with a Nikon Eclipse E-200 POL polarizing microscope (Tokyo, Japan). Samples were put between glass slides. Microphotographs were taken without crossed polarizers.

REFERENCES

1. Chang, M. C.; Ko, C.-C.; Douglas, W. H. Biomaterials 2003, 24, 2853–2862.
2. Deshpande, A. S.; Beniash, E. Crystal Growth Des 2008, 8, 3084–3090.
3. Zheng, W.; Zhang, W.; Jiang, X. Adv Eng Mater 2010, 12, B451–B466.
4. Liu, Y.; Li, N.; Qi, Y.-p.; Dai, L.; Bryan, T. E.; Mao, J.; Pashley, D. H.; Tay, F. R. Adv Mater 2011, 23, 975–980.
5. Goissis, G.; Da Silva Maginador, S. V.; Da Conceição Amaro Martins, V. Artificial Organs 2003, 27, 437–443.
6. Mehlisch, D. R.; Leider, A. S.; Eugene Roberts, W. Oral Surg Oral Med Oral Pathol 1990, 70, 685–692.
7. Miyamoto, Y.; Ishikawa, K.; Takechi, M.; Toh, T.; Yuasa, T.; Nagayama, M.; Suzuki, K. Biomaterials 1998, 19, 707–715.
8. Niu, L.-N.; Jiao, K.; Ryou, H.; Yiu, C. K. Y.; Chen, J.-H.; Breschi, L.; Arola, D. D.; Pashley, D. H.; Tay, F. R. Angewandte Chemie Int Ed 2013, 52, 5762–5766.
9. Pederson, A. W.; Ruberti, J. W.; Messersmith, P. B. Biomaterials 2003, 24, 4881–4890.
10. TenHuisen, K. S.; Martin, R. I.; Klimkiewicz, M.; Brown, P. W. J Biomed Mater Res 1995, 29, 803–810.
11. Zhang, W.; Liao, S. S.; Cui, F. Z. Chem Mater 2003, 15, 3221–3226.
12. Hartgerink, J. D.; Beniash, E.; Stupp, S. I. Science 2001, 294, 1684–1688.
13. Magne, D.; Weiss, P.; Bouler, J.-M.; Laboux, O.; Daculsi, G. J Bone Mineral Res 2001, 16, 750–757.
14. Hassan, N.; Soltero, A.; Pozzo, D.; Messina, P. V.; Ruso, J. M. Soft Matter 2012, 8, 9553–9562.
15. Messina, P. V.; Hassan, N.; Soltero, A.; Ruso, J. M. RSC Adv 2013, 3, 24256–24265.
16. D'Elía, N. L.; Gravina, A. N.; Ruso, J. M.; Laiuppa, J. A.; Santillán, G. E.; Messina, P. V. Biochimica; Biophysica Acta (BBA) - General Subjects 2013, 1830, 5014–5026.
17. Deville, S.; Saiz, E.; Tomsia, A. P. Biomaterials 2006, 27, 5480–5489.
18. Kim, H.-W.; Kim, H.-E.; Salih, V. Biomaterials 2005, 26, 5221–5230.
19. Landi, E.; Valentini, F.; Tampieri, A. Acta Biomaterialia 2008, 4, 1620–1626.
20. Lu, Y.; An, L.; Wang, Z.-G. Macromolecules 2013, 46, 5731–5740.
21. Masuelli, M. A.; Sansone, M. G. In Products and applications of biopolymers; Verbeek, D. J., Ed.; InTech, 2012, p 85–116.
22. Liu, J.; Nguyen, M. D. H.; Andya, J. D.; Shire, S. J. J Pharma Sci 2005, 94, 1928–1940.
23. Nishida, K.; Kaji, K.; Kanaya, T.; Fanjat, N. Polymer 2002, 43, 1295–1300.
24. Kraemer, E. O.; Lansig, W. D. J Phys Chem 1934, 39, 153–168.
25. Schulz, G. V.; Blaschke, F. J Prakt Chem 1941, 158, 130–135.
26. Martin, A. F. TAPPI 1951, 34, 363–366.
27. Huggins, M. L. J Am Chem Soc 1942, 64, 2716–2718.
28. Li, Y.; Cheng, R. J Polym Sci B: Polym Phys 2006, 44, 1804–1812.
29. Nishida, K.; Kaji, K.; Kanaya, T. Polymer 2001, 42, 8657–8662.
30. Lewandowska, K.; Staszewska, D. U.; Bohdanecký, M. Eur Polym J 2001, 37, 25–32.
31. Barth, H. G.; Mays, J. W., Eds. Modern Methods of Polymer Characterization; Wiley, 1991, New York.
32. Puvvada, N.; Panigrahi, P. K.; Pathak, A. Nanoscale 2010, 2, 2631–2638.
33. Peng, S.; Wu, C. Polymer 2001, 42, 7343–7347.
34. Peng, S.; Wu, C. Macromolecules 2001, 34, 6795–6801.
35. Lin, W.; Zhou, Y.; Zhao, Y.; Zhu, Q.; Wu, C. Macromolecules 2002, 35, 7407–7413.
36. Vlachy, N.; Jagoda-Cwiklik, B.; Vácha, R.; Touraud, D.; Jungwirth, P.; Kunz, W. Adv Colloid Interface Sci 2009, 146, 42–47.
37. Zhang, Y.; Cremer, P. S. Current Opin Chem Biol 2006, 10, 658–663.
38. Pan, Y.; Cheng, R.-S. Chinese J Polym Sci (CJPS) 2000, 18, 57–67.

39. Harding, S. E. Prog Biophys Mol Biol 1997, 68, 207–262.
40. El-Sherbiny, I. M.; Smyth, H. D. C. J Nanomater 2011, 2011.
41. Muhidinov, Z. K.; Fishman, M. L.; Avloev, K. K.; Norova, M. T.; Nasriddinov, A. S.; Khalikov, D. K. Polym Sci Ser A 2010, 52, 1257–1263.
42. Messina, P. V.; Prieto, G.; Ruso, J. M.; Sarmiento, F. J Phys Chem B 2005, 109, 15566–15573.
43. Abrusci, C.; Martín-González, A.; Amo, A. D.; Catalina, F.; Bosch, P.; Corrales, T. J Photochem Photobiol A: Chem 2004, 163, 537–546.
44. Herrmann, K. L.; McCulloch, A. D.; Omens, J. H. Am J Physiol Heart Circ Physiol 2003, 284, H1277–H1284.
45. Oliveira, A. L.; Sun, L.; Kim, H. J.; Hu, X.; Rice, W.; Kluge, J.; Reis, R. L.; Kaplan, D. L. Acta Biomaterialia 2012, 8, 1530–1542.
46. Corriu, R. J. P.; Embert, F.; Guari, Y.; Mehdi, A.; Reye, C. Chem Commun 2001, 1116–1117.
47. Brown, J.; Richer, R.; Mercier, L. Microporous Mesoporous Mater 2000, 37, 41–48.

Reviewing Editor: C. Allen Bush